Journal of The Physical Society of Japan
Vol. 61, No. 8, August, 1992, pp. 2748–2753

Cross Sections of Charge Exchange for Fast He Ions Passing through Zn Vapor

Manabu SAITO,* Makoto IMAI,** Koji IWASAWA,
Naoki SAKURA, Nobutsugu IMANISHI and Fumio FUKUZAWA***

Department of Nuclear Engineering, Faculty of Engineering,
Kyoto University, Kyoto 606

(Received January 7, 1992; revised manuscript received April 20, 1992)

Single and double electron loss and capture cross sections have been measured for He^0, He^{1+} and He^{2+} ions passing through a Zn vapor target at energies ranging from 0.8 to 2.0 MeV. Uncertainties of the cross sections were improved by applying the Rutherford scattering method for the determination of the target thickness. When combined with other previous experimental data, obtained cross sections support the oscillatory dependence on target atomic number. In addition, the equilibrium mean charges of He ions were compared for solid and gas phases of the Zn element, but no density effect has been observed.

[charge exchange, zinc vapor, Rutherford scattering method, target thickness, oscillatory dependence, density effect]

§1. Introduction

Charge exchange cross sections for fast He ions have been measured by several groups.[1–6] However, data are still insufficient to discuss an oscillatory dependence of the single-electron capture cross section on atomic number or to clarify a density effect of the equilibrium mean charge.

As to the oscillatory dependence, it has been unambiguously observed for the equilibrium mean charge for solid.[7,8] It is believed that the dependence reflects the behavior of the capture cross section. Most of the capture cross sections, however, have been measured for gas targets, whose atomic numbers are almost limited to values below 18. Therefore, it is required to obtain data for various vaporized metals.

Again the density effect of the equilibrium mean charge, almost all previous comparisons have been made between solid carbon and oxygen or nitrogen gas.[9] As noted above, the equilibrium mean charge depends on atomic number in an oscillatory manner. Then, the equilibrium mean charge has to be compared between gas and solid phases of the same element for the precise study of the density effect.

On the contrary, experiments have been scarce for vapor targets because of difficulty in precise determination of the target thickness. So far, the thickness has been obtained in general from a vapor pressure multiplied by an effective target length. But one meets many difficulties in measuring both parameters, which made it difficult to obtain accurate cross sections.

In the present experiments, we have improved the accuracy of the vapor-target thickness by applying the Rutherford scattering method, and measured absolute cross sections of charge exchange for He ions on Zn vapor target in an energy range of 0.8–2.0 MeV. The obtained data are compared with previous experimental data for gas targets[1–6] and with theoretical treatments.[10–14] In addition, the density effect is examined unambiguously by comparing the experimental values of equilibrium mean charge of He ions through the solid and vapor phases of the same element.

* Present address: Laboratory of Applied Physics, Kyoto Prefectural University.
** Present address: Tokai Research Establishment, Japan Atomic Energy Research Institute.
*** Present address: Okayama Polytechnic College.

§2. Experimental

2.1 Measurements of target thickness

In the present experiment, the measurements of the thickness of the Zn vapor target were done in separate runs before the data accumulation of the charge fractions.

Figure 1 shows a schematic of the experimental apparatus for the measurement of the target thickness by the Rutherford scattering method. He^+ ions accelerated with a Van de Graaff accelerator of Kyoto University were collimated with a circular slit 0.9 mm in diam. and led into the vapor column. He ions scattered by Zn atoms were detected with a surface barrier semiconductor detector (SSD) set at an angle of $3.98° \pm 0.07°$. Here, Zn vapor was evaporated from a quartz oven heated with a tungsten coil and was trapped on a water-cooled copper covering over the oven. The atomic density of the vapor was kept constant by controlling the temperature of liquid Zn with a chromel-alumel thermocouple inserted in the oven.

Data of the incident beam current and the number of scattered ions were taken at several liquid temperatures between 723 K and 793 K. The liquid Zn temperature was recorded during the experiment at an interval of 6.4 sec to inspect its variation, which was found to be less than ± 0.5 K. The chamber pressure was also monitored in order to estimate a background contribution. In §3.1, the data will be analyzed to obtain the target thickness of vapor Zn column at the temperatures. In the analyses, the precise energy of the incident He ions is required to calculate the Rutherford scattering cross section. Then, the energy was determined as 1.00 ± 0.04 MeV using a 90° analyzing magnet whose magnetic field was calibrated beforehand by the $^{27}Al(p, \gamma)^{28}Si$ resonance method. The typical beam current was 10 nA, which was monitored with a Faraday cup, and was corrected the mean charge of the He ions after passing through the vapor. Here, the mean charge was measured by the method described in the next sub section.

2.2 Measurements of charge fractions

In the measurements of charge fractions of He ions, the Faraday cup was removed and a position sensitive semiconductor detector (PSD) was set at the location of the cup as shown in Fig. 1. He^+ ions analyzed with the calibrated 90° analyzing magnet collided with residual gases before reaching the vapor target and changed their charge states. A given charge state therefore was separated from the others by passing through a charge selector composed of four magnetic deflectors and three slits. The charge-selected beam whose purity was at least 98% was collimated with a hole slit of 0.9 mm in diam. and led into the center of Zn vapor column mentioned in §2.1. The ions which passed through the vapor column were separated magnetically according to the respective charge states and detected with the PSD.

The energy and position signals were taken into a two-parameter multichannel analyzer.

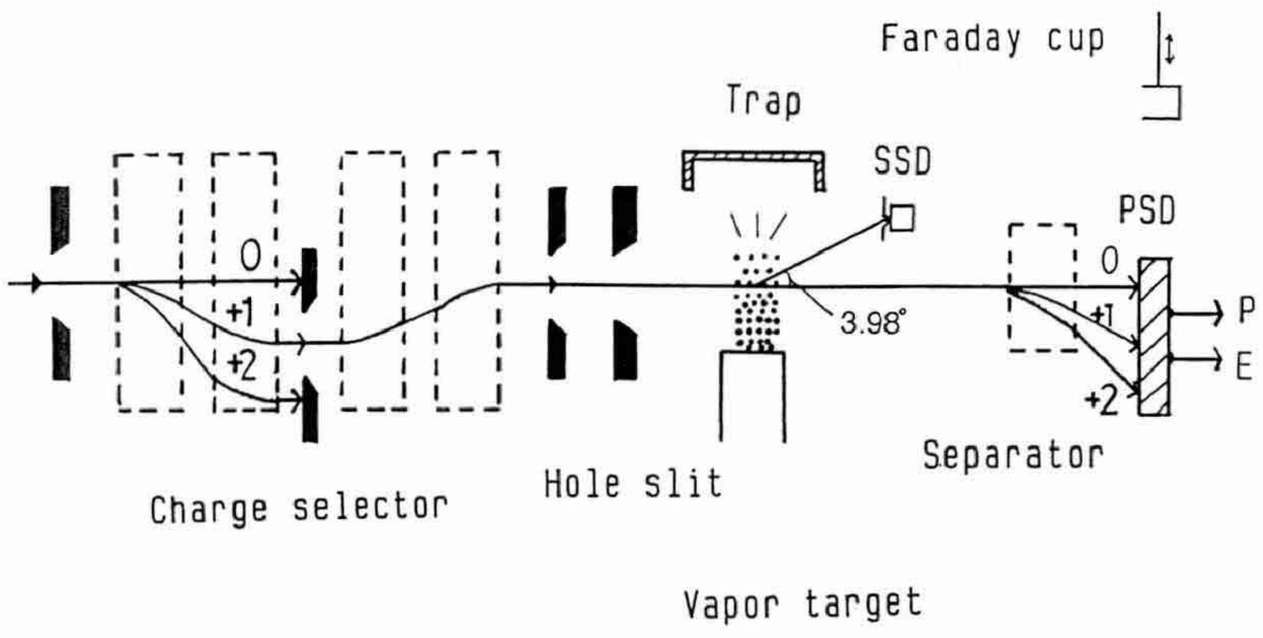

Fig. 1. Experimental set-up for the measurements of target thickness and charge fractions.

The temperature of the liquid Zn in the oven and the pressure in the target chamber were recorded to obtain the vapor-thickness and to correct background, respectively. The charge fractions of He ions were measured at energies of 0.8, 1.0, 1.2, 1.5 and 2.0 MeV.

§3. Analysis

3.1 Target thickness

In order to obtain the target thickness π of the Zn vapor column, yields Y_s of scattered ion per incident particle were measured at the temperatures T of the liquid Zn in the oven. Then the yield Y_s at a given temperature is described by the following equation, as far as the target thickness is low enough:

$$Y_s=\int \sigma_s(x)P(x)\,dx+Y'_s, \qquad (1)$$

where $P(x)$ is the density of vapor at a point x along the beam axis, $\sigma_s(x)$ is the Rutherford scattering cross section and Y'_s is a background contribution from gases other than vapor column.

As the vapor density is expressed by a Gaussian function, eq. (1) can be accurately approximated as

$$Y_s=\sigma_s\pi+Y'_s, \qquad (2)$$

where σ_s is the calculated Rutherford scattering cross section at the incident energy of 1.00 MeV for the scattering angle of 3.98°. In the analysis, the background correction was assumed to be constant at temperatures above 723 K. Then eq. (2) can be written as

$$\pi(T)-\pi(723)=(Y_s(T)-Y_s(723))/\sigma_s. \qquad (3)$$

The constant correction was reliable because the chamber pressure increased quickly from a value of 1.3×10^{-4} to 2×10^{-3} Pa with increasing liquid Zn temperature from 300 K to 723 K, but the pressure settled above 723 K.

The thickness obtained thus is free of vapor pressure and shape of vapor column. The uncertainty was estimated to be within 8% which are due to the statistical error 1% and the uncertainty 7% of the scattering cross section due to the span of the scattering angle. Previous charge-exchange cross section for vapor targets[15-18] were troubled by large uncertainties of vapor thickness ranging from 13 to 20%.

3.2 Cross sections of charge exchange

In the single collision approximation, the yield Y_{if} of ions changing their charges from i to f is given by

$$Y_{if}=\sigma_{if}\pi+Y'_{if}, \qquad (4)$$

where i and f are the respective initial and final charge states, σ_{if} the electron loss or capture cross section, π the target thickness, and Y'_{if} the background contribution. The background was corrected by the method as mentioned in §3.1. Then, eq. (4) can be written as

$$(Y_{if}(T)-Y_{if}(723))=\sigma_{if}(\pi(T)-\pi(723)). \qquad (5)$$

Cross sections σ_{if} were then deduced from the growth curves by the least-squares-method. Figure 2 shows examples of the typical growth curves. Inclusion of a quadratic term did not improve the fitting any more. Therefore, the two-step collision process contributed little.

3.3 Equilibrium mean charge

For the case of three charge states, the equilibrium mean charge q is given by the following formula:

$$q=[(\sigma_{01}+\sigma_{02})(\sigma_{21}+2\sigma_{12})+\sigma_{01}\sigma_{20}+2\sigma_{02}\sigma_{10}]/D, \qquad (6)$$

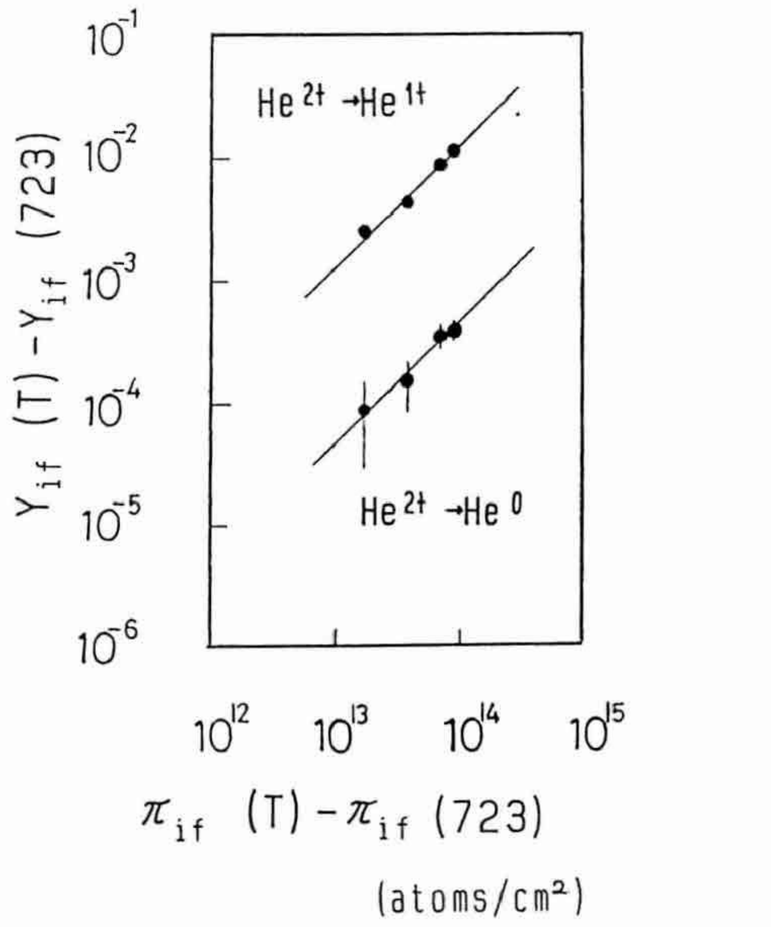

Fig. 2. Growth curves of 1.0 MeV of He^{2+} ions for the Zn vapor target.

where D is

$$D=(\sigma_{01}+\sigma_{02})(\sigma_{21}+\sigma_{12})+(\sigma_{02}+\sigma_{21})\sigma_{10}+(\sigma_{01}+\sigma_{10}+\sigma_{12})\sigma_{20},$$

where the cross sections for He^{1-} ions is not included because it is too low to be measured.

§4. Results and Discussion

Table I shows the cross sections σ_{if} of charge changing collisions for He^0, He^{1+} and He^{2+} incident on Zn. Experimental errors include the uncertainty of target thickness in addition to statistical errors.

Figure 3 shows the obtained loss and capture cross sections plotted as a function of energy. So far, no measurement has been reported for the $He^{i+}+Zn$ collision. Therefore, our data are compared with ones for Kr measured by Pivovar *et al.*[1,2] and by Hvelplund *et al.*[3] The cross sections for Zn show a similar energy dependence as those for Kr, but absolute values for Zn are much larger than those for Kr. The cross section ratios of Zn to Kr are 3~4, 2~6 and 2 for the single capture, double capture and loss, respectively.

The experimental cross sections σ_{21}[2,4,5,19] of single electron capture for 1.0 MeV He^{2+} are shown in Fig. 4. The calculated values of the OBK approximation[10,11] and of the Bohr-Lindhard model[12,13] are also plotted in the figure. The OBK values were normalized to the experimental value at the Ar point. As known from Fig. 4, both calculations predict oscillatory dependences of the capture cross section σ_{21} on the target atomic number Z_t.

Table I. Cross sections (10^{-16} cm^2) and equilibrium mean charges of He ions for Zn vapor target.

E (MeV)	σ_{01}	σ_{02}	σ_{12}	σ_{10}	σ_{21}	σ_{20}	q
0.8	5.02±0.77	0.74±0.17	2.22±0.24	0.38±0.06	1.99±0.26	0.081±0.026	1.47±0.04
1.0	5.42±0.60	0.84±0.12	2.26±0.30	0.23±0.05	1.28±0.17	0.045±0.015	1.61±0.04
1.2	5.19±0.57	0.85±0.12	2.72±0.31	0.19±0.04	1.14±0.12	0.021±0.009	1.68±0.03
1.5	5.48±0.69	0.56±0.12			0.62±0.09	0.009±0.008	
2.0	6.31±0.75	0.85±0.15	2.36±0.28	0.064±0.019	0.44±0.07	0.006±0.006	1.84±0.03

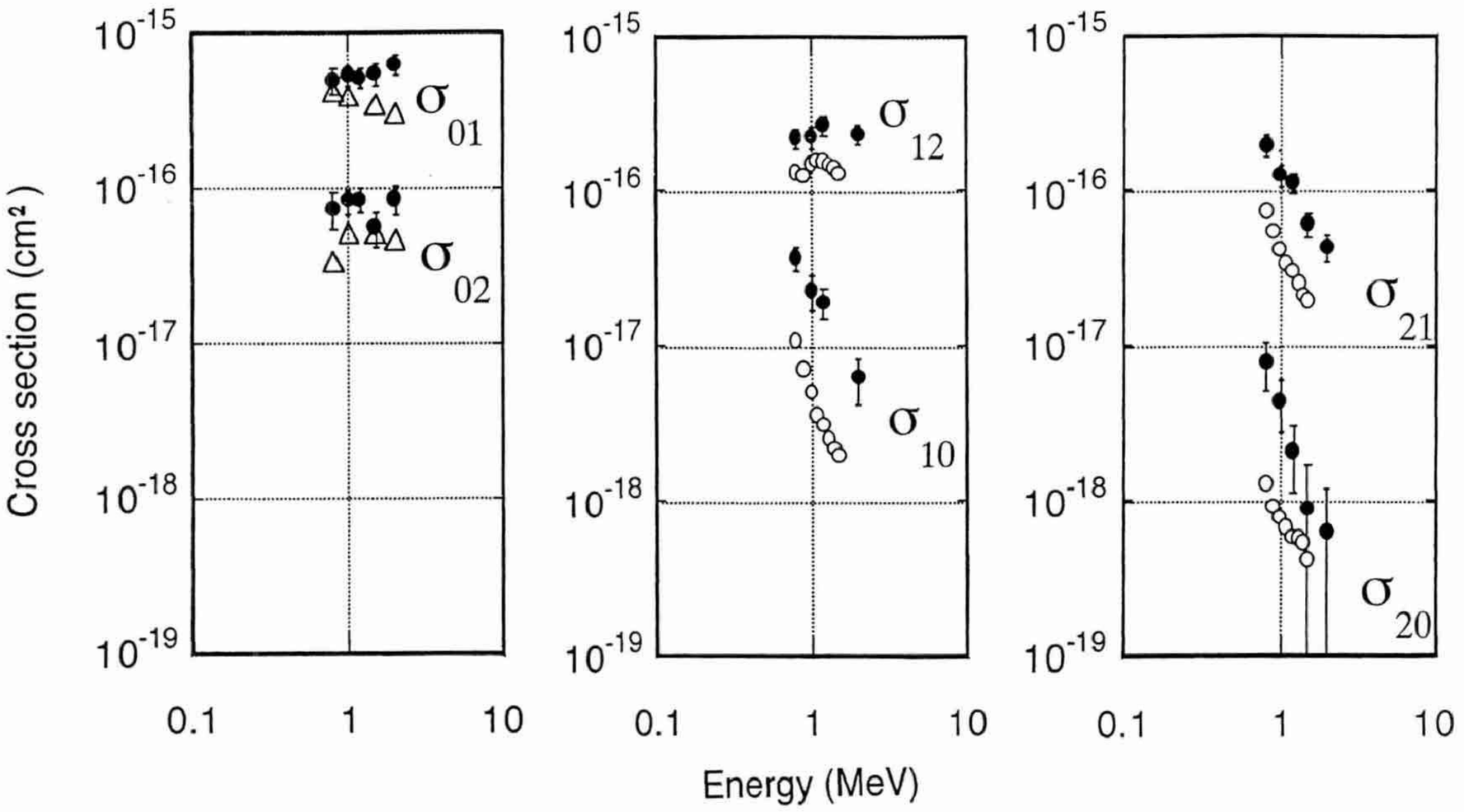

Fig. 3. Charge exchange cross sections of He ions; ●: this work for Zn target; ○: Kr target by Pivovar *et al.*;[1,2] △: Kr target by Hvelplund *et al.*[3]

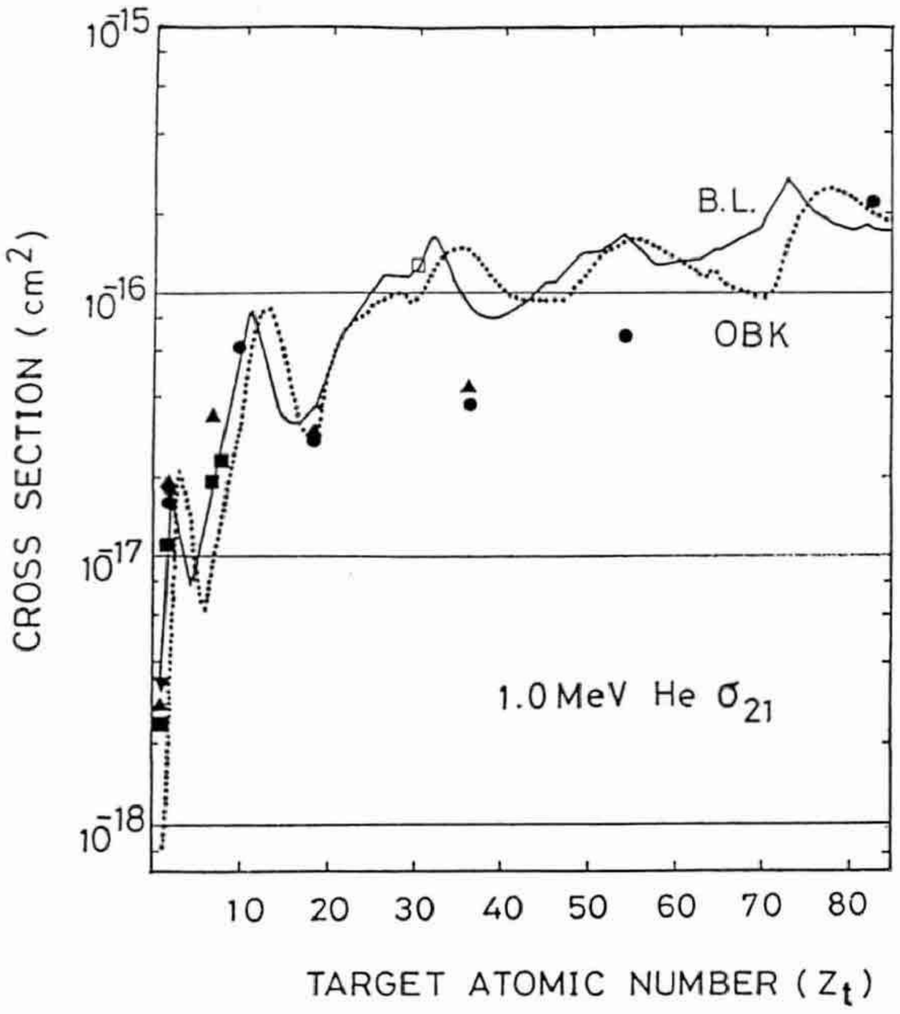

Fig. 4. Electron capture cross sections for 1.0 MeV He ion. Experimental values are marked as; □ present data, ▲ Pivovar *et al.*,[2] ▼ Hvelplund *et al.*,[4] ■ Itoh *et al.*,[5] ● Kanamori *et al.*[19] A solid and a dotted line denote σ_{21} calculation of Bohr-Lindhard and of OBK, respectively.

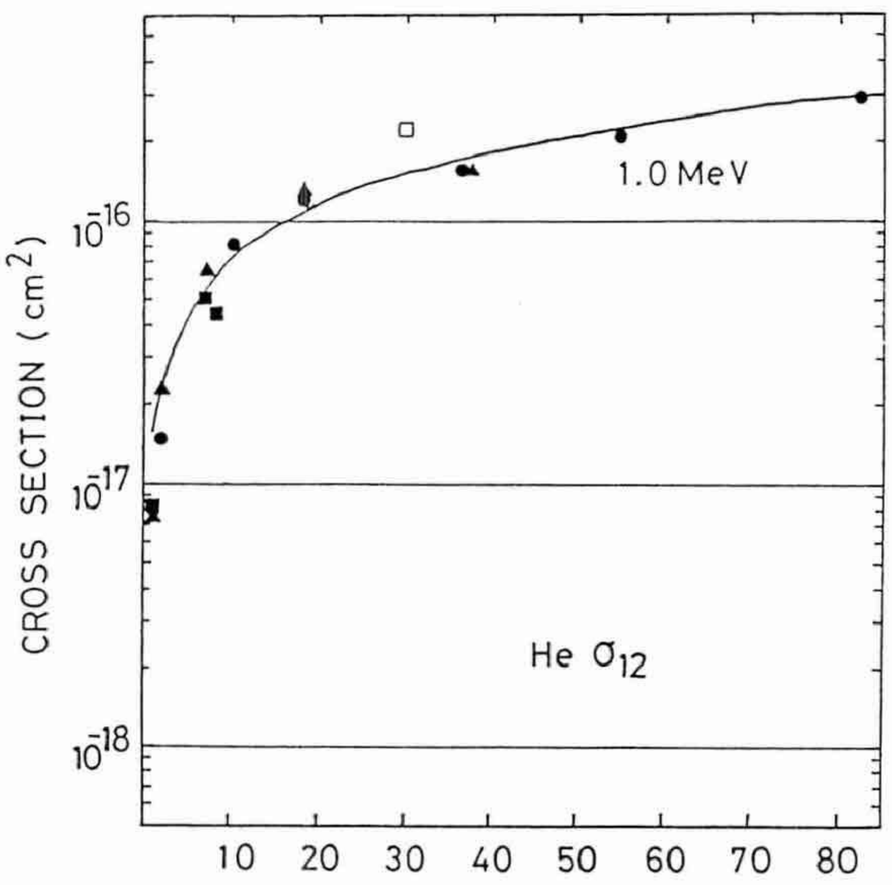

Fig. 5. Electron loss cross sections of 1.0 MeV He ion. Experimental values are marked as; □ present data, ▲ Pivovar *et al.*,[1] ■ Itoh *et al.*,[6] ● Kanamori *et al.*[19] A solid line denotes σ_{12} calculation of Bohr.

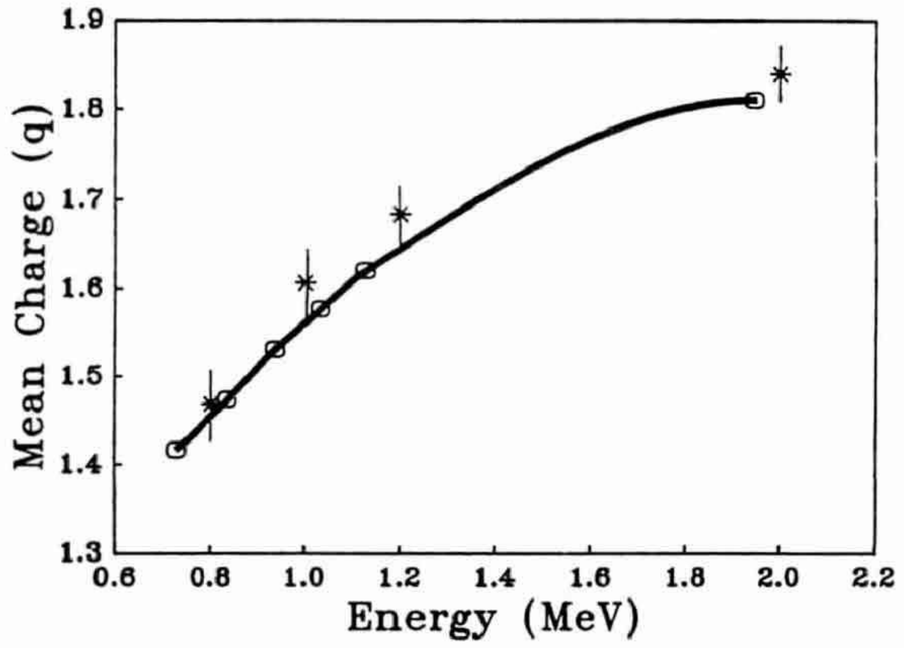

Fig. 6. Equilibrium mean charges of He ions for Zn are compared between vapor and solid; ∗: present data for vapor; ○: data for solid.[7] A solid line is drawn to guide the eye.

The experimental data support the predicted dependence for the atomic number below 18. Above 18, however, data have been scarce to compare with the predictions. The obtained result for Zn are much larger than both the values for Ar and Kr. The fact partly supports the hump of the cross section predicted between Ar and Kr.

Figure 5 shows the experimental single electron loss cross sections σ_{12}[1,6,19] at 1.0 MeV and the values calculated on the assumption of $Z_t^{2/3}$ dependence.[14] The experimental data are in agreement with the assumption. But the σ_{12} for Zn is slightly larger than the $Z_t^{2/3}$ curve by a factor of 1.6.

Double electron capture and loss cross sections σ_{20} and σ_{02} tend to increase with increasing target number so far as rare gases are concerned. However, it has been found that values for Zn are larger than those for Ar and Kr.[2,3] The cross section ratios of Zn to Ar or Kr are 6 and 1.5 for the double capture and double loss at 1.0 MeV, respectively. The experimental result indicates the oscillatory dependence of double capture on Z_t.

The equilibrium mean charges of He ions for Zn vapor are presented in Table I. Figure 6 compares the values for vapor and solid.[7] Both values for vapor and solid agree with each other within experimental errors. Thus, the density effect is not observed for fast He ions incident on the Zn targets with different phases. The fact means that the excited states

in He^+ is hardly populated in the solid Zn because of large radii of the excited states.

Acknowledgment

We would like to thank Professor M. Tomita, Professor Y. Haruyama, Mr. K. Yoshida, Mr. K. Norisawa and Mr. T. Ohdaira for many useful discussions and help in data taking.

References

1) L. I. Pivovar, M. T. Novikov and V. M. Tubaev: Sov. Phys.-JETP **14** (1962) 20.
2) L. I. Pivovar, M. T. Novikov and V. M. Tubaev: Sov. Phys.-JETP **15** (1962) 1035.
3) P. Hvelplund and E. H. Pedersen: Phys. Rev. **A9** (1974) 2434.
4) P. Hvelplund, J. Heinemeier, E. H. Pedersen and F. R. Simpson: J. Phys. **B9** (1976) 491.
5) A. Itoh, M. Asari and F. Fukuzawa: J. Phys. Soc. Jpn. **48** (1980) 943.
6) A. Itoh, K. Ohnishi and F. Fukuzawa: J. Phys. Soc. Jpn. **49** (1980) 1513.
7) Y. Haruyama: Ph. D. Thesis, Kyoto University, Kyoto, Japan.
8) K. Shima, T. Ishihara, T. Momoi, T. Miyoshi, K. Numata and T. Mikumo: Phys. Lett. **98A** (1983) 106.
9) H. D. Betz: Rev. Mod. Phys. **44** (1972) 465.
10) M. R. C. Mcdowell and J. P. Coleman: *Introduction to the Theory of Ion-Atom Collisions* (North-Holland Pub. Com., Amsterdam, 1970) p. 373.
11) V. S. Nikolaev: Sov. Phys.-JETP **24** (1967) 847.
12) N. Bohr and J. Lindhard: K. Dan. Vidensk. Selsk. Mat.-Fys. Medd. **28** (1954) 7.
13) A. Itoh, Y. Haruyama, Y. Kanamori, T. Kido and F. Fukuzawa: Bulletin of the Chem. Research, Kyoto Univ. **60** (1982).
14) N. Bohr: K. Dan. Vidensk. Selsk. Mat.-Fys. Medd. **18** (1948) 8.
15) R. W. McCullough, T. V. Goffe, M. B. Shah, M. Lennon and H. B. Gilbody: J. Phys. **B15** (1982) 111.
16) S. L. Varghese, W. Waggoner and C. L. Cocke: Phys. Rev. **A29** (1984) 2453.
17) R. D. DuBois and L. H. Toburen: Phys. Rev. **A31** (1985) 3603.
18) R. D. DuBois: Phys. Rev. **A32** (1985) 3319.
19) Y. Kanamori *et al.*: private communication.